東北大学機関リポジトリ
TOUR
Tohoku University Repository

Light polarization characteristics of m-plane AlxGa1-xN films suffering from in-plane anisotropic tensile stresses

著者	Hazu K., Hoshi T., Kagaya M., Onuma T., Chichibu S. F.
journal or publication title	Journal of Applied Physics
volume	107
number	3
page range	033701
year	2010
URL	http://hdl.handle.net/10097/52436

doi: 10.1063/1.3282705

Light polarization characteristics of *m*-plane $Al_xGa_{1-x}N$ films suffering from in-plane anisotropic tensile stresses

K. Hazu,[a] T. Hoshi, M. Kagaya, T. Onuma, and S. F. Chichibu[b]
CANTech, Institute of Multidisciplinary Research for Advanced Materials, Tohoku University, 2-1-1 Katahira, Aoba, Sendai 980-8577, Japan

(Received 15 September 2009; accepted 2 December 2009; published online 1 February 2010)

Polarization characteristics of the near-band-edge optical transitions in *m*-plane $Al_xGa_{1-x}N$ epilayers suffering from anisotropic stresses were quantified. The epilayers were grown by both ammonia-source molecular beam epitaxy and metalorganic vapor phase epitaxy methods on an *m*-plane freestanding GaN substrate. The light polarization direction altered from $E \perp c$ to $E \parallel c$ at the AlN molar fraction, x, between 0.25 and 0.32, where E is the electric field component of the light and $\perp$ and $\parallel$ represent perpendicular and parallel, respectively. To give a quantitative explanation for the result, energies and oscillator strengths of the exciton transitions involving three separate valence bands were calculated as functions of strains using the Bir–Pikus Hamiltonian. The calculation predicted that the lowest energy transition (E_1) is polarized to the *m*-axis normal to the surface (X_3) for $0 < x \leq 1$, meaning that E_1 emission is principally undetectable from the surface normal for any in-plane tensile strained $Al_xGa_{1-x}N$. The polarization direction of observable surface emission was predicted to alter from *c*-axis normal (X_1) to *c*-axis parallel (X_2) for the middle energy transition (E_2) and X_2 to X_1 for the highest energy transition (E_3) between $x=0.25$ and 0.32. The experimental results were consistently reproduced by the calculation. *© 2010 American Institute of Physics*. [doi:10.1063/1.3282705]

I. INTRODUCTION

Wurtzite $Al_xGa_{1-x}N$ alloys are an attractive material for realizing ultraviolet light emitters and high power high frequency electronic devices, as their bandgap energies range from 3.43 eV ($x=0$) to 6.01 V ($x=1$) and they are principally a hard material. Recently, a 210 nm electroluminescence has been demonstrated for *c*-plane AlN *p-i-n* homojunction light-emitting diodes (LEDs),[1] although the external quantum efficiency (10^{-6}% at 210 nm) was extremely lower than those of conventional blue or violet InGaN LEDs. One of the major reasons for this is the increase in threading dislocation (TD) and point defect densities[2] with the increase in AlN molar fraction x. Another reason is the reduction in oscillator strength of electron-hole pairs in quantum wells (QWs) due to the quantum-confined Stark effects (QCSEs), which are caused by the spontaneous and piezoelectric polarization discontinuity at the *c*-plane heterointerfaces. To avoid the QCSEs in (Al, In, Ga)N heterostructures, epitaxial growths on nonpolar orientations such as *a*-plane $(11\bar{2}0)$ or *m*-plane $(10\bar{1}0)$ have been attracting attention.[3–6] Recently, good performance *m*-plane InGaN LEDs[7,8] and LDs[9,10] have been fabricated on the low TD density freestanding (FS)-GaN substrates,[11] which were sliced from a subcentimeter-thick *c*-plane FS-GaN grown by halide vapor phase epitaxy. However, for nonpolar epitaxy of (Al, In, Ga)N alloys, in-plane lattice and thermal mismatches between the epilayer and the substrate are anisotropic along parallel and normal to the *c*-axis, which gives rise to anisotropic strains in the pseudomorphic epitaxial films. Therefore, in order to optimize nonpolar $Al_xGa_{1-x}N$ LED structures, oscillator strengths f of three interband optical transitions must be quantified as functions of light polarization direction and strains.

The effects of biaxial isotropic strain on excition resonance energies have been investigated for *c*-plane GaN (Refs. 12–14) and *c*-plane AlN.[15] Because the sign of the crystal-field splitting of AlN is negative, valence band (VB) ordering of strain-free AlN is Γ_7, Γ_9, and Γ_7 in order of decreasing electron energy. On the other hand, the ordering is Γ_9, Γ_7, and Γ_7 for GaN and InN. Consequently, the allowed light polarization direction for the topmost VB of $Al_xGa_{1-x}N$ alters from $E \perp c$ to $E \parallel c$ with the increase in x, where E is the electric field of the light and $\perp$ and $\parallel$ represent perpendicular and parallel, respectively. Ikeda *et al.*[15] have obtained the VB parameters of AlN through the theoretical fitting of exciton transition energies of *c*-plane AlN films as a function of biaxial strain. As a result, they have predicted the critical x (anticrossing point) for the A and C transitions as 0.125.

With respect to the effect of anisotropic strains, optical polarization properties of (Al, In, Ga)N films and QWs of various orientations have been investigated.[16–26] Bhattacharyya *et al.*[26] have very recently calculated the light polarization characteristics of the transitions involving three separate VBs of *m*-plane $Al_xGa_{1-x}N$ on GaN, which suffer form anisotropic tensile stresses. They have estimated the anticrossing point as $x=0.10$, and predicted that the lowest energy transition of $Al_xGa_{1-x}N$ is predominantly polarization parallel to the substrate normal.

In this paper, results of polarized cathodoluminescence (CL) measurement on *m*-plane $Al_xGa_{1-x}N$ epilayers grown

[a]Electronic mail: k_hazu@tagen.tohoku.ac.jp.
[b]Electronic mail: chichibulab@yahoo.co.jp.

 © 2010 American Institute of Physics

Downloaded 31 Aug 2011 to 130.34.134.250. Redistribution subject to AIP license or copyright; see http://jap.aip.org/about/rights_and_permissions

on the m-plane FS-GaN substrate are shown. All of the epilayers grown by ammonia-source molecular beam epitaxy (NH_3-MBE) and metalorganic vapor phase epitaxy (MOVPE) suffer from in-plane anisotropic tensile stresses. The results are quantitatively explained by calculating transition energies and oscillator strengths of excitonic transitions involving three separate VBs as functions of in-plane strains. For the calculation, Bir–Pikus Hamiltonian[27] was used without fitting parameters.

II. EXPERIMENTAL DETAILS

Samples investigated were approximately 100 to 400-nm-thick m-plane $Al_xGa_{1-x}N$ epilayers grown on an 1-μm-thick GaN homoepitaxial layer, which was grown on the m-plane FS-GaN substrates.[11] The substrates were sliced form approximately 1-cm-thick c-plane FS-GaN grown by halide vapor phase epitaxy on a Al_2O_3 substrate.[11] The TD and stacking fault densities were lower than 5×10^6 cm^{-2} and 1×10^3 cm^{-1}, respectively.[11] The NH_3-MBE of m-plane $Al_xGa_{1-x}N$ epilayers ($0\leq x\leq0.70$) were carried out at 870–970 °C using metallic Ga (7N) and Al (6N) sources. The beam equivalent pressures of metallic Ga and NH_3 were $(2.1-4.0)\times10^{-5}$ and $(1.3-4.1)\times10^{-2}$ Pa, respectively. The growth details will be found in Ref. 28. A 150-nm-thick $Al_{0.73}Ga_{0.27}N$ and approximately 2.1-μm-thick AlN epilayers were grown at 1120 °C on the same m-plane FS-GaN substrates by MOVPE. The reactor pressure was 2.02×10^4 Pa. Trimethylaluminum, triethylgallium, and NH_3 were used as the precursors.

The $Al_xGa_{1-x}N$ films of $0\leq x\leq0.32$ were confirmed by x-ray reciprocal space mapping (RSM) method to grow coherently on the base GaN. The films of $x>0.58$ were incompletely relaxed because of the lattice mismatch against the GaN substrate.[28] Accordingly, two in-plane and one out-of-plane strains and x values were obtained from the in-plane and out-of-plane lattice parameters measured by the x-ray RSM measurement, taking the degree of lattice relaxation into account.[28] In-plane tensile strains increased with x for the pseudomorphic (coherently grown) films, as shown in Fig. 1(a). Conversely, the strains were gradually relaxed by the partial relaxation for $x>0.32$. For the quantitative discussion of polarization properties, we define the notations for the three axes: X_1 (perpendicular to the c-axis in the growth plane), X_2 (parallel to the c-axis in the growth plane), and X_3 (normal to the growth plane), as shown in Fig. 1(b).

Steady-state CL was excited with an electron beam operated at 3.0 kV. The probe current density was 1.0×10^{-2} A/cm^2 at sample. The emission was dispersed by a 30-cm-focal-length grating monochromator, and detected using a multichannel charge-coupled device. A Glan–Thompson prism polarizer was used for the polarized CL measurement. Polarized near-band-edge (NBE) CL spectra at 12 K of the m-plane $Al_xGa_{1-x}N$ films are shown as a function of x in Fig. 2(a). The intensities are normalized to that of stronger polarization direction (X_1 or X_2) for each x. The entire spectra shifted to the higher energy with increasing x, although some of them exhibited double emission peaks. As shown, the light polarization direction altered from X_1 to X_2 between $x=0.25$ and 0.32. The value of polarization ratio ρ was defined as $(I_{X_1}-I_{X_2})/(I_{X_1}+I_{X_2})$, where I_{X_2} and I_{X_1} are the spectrally integrated CL intensities of the NBE emission. The values are plotted by closed circles in Fig. 2(b).

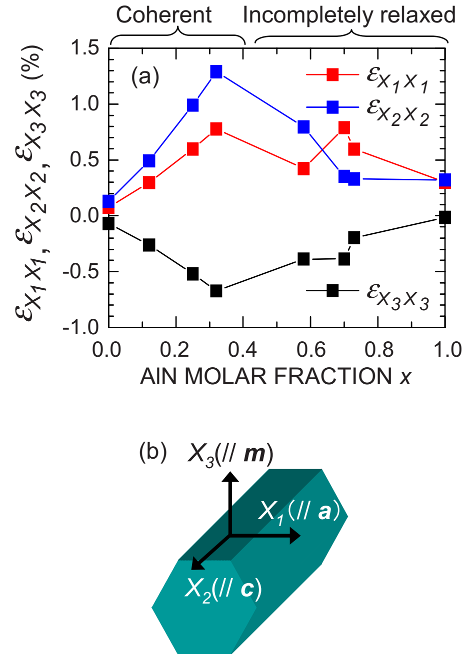

FIG. 1. (Color online) (a) Strain components $\epsilon_{X_1X_1}$, $\epsilon_{X_2X_2}$, and $\epsilon_{X_3X_3}$ of the m-plane $Al_xGa_{1-x}N$ films as a function of AlN molar fraction x. (b) Schematic diagram of the notations of three axes. The films of $x\leq0.70$ were grown by NH_3-MBE and $x\geq0.73$ were grown by MOVPE.

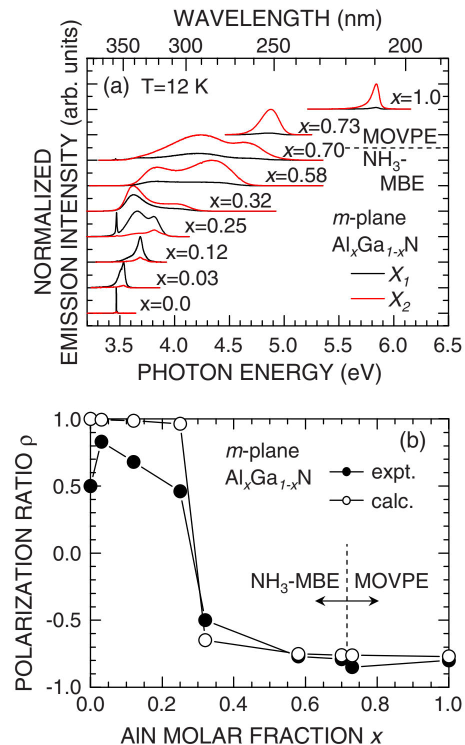

FIG. 2. (Color online) (a) Polarized CL spectra at 12 K of m-plane $Al_xGa_{1-x}N$ epilayers grown on the FS m-plane GaN substrates. (b) Polarization ratios, which are defined as $(I_{X_1}-I_{X_2})/(I_{X_1}+I_{X_2})$, of the $Al_xGa_{1-x}N$ films as a function of AlN molar fraction x. Corresponding values calculated using the relative oscillator strengths are also shown. The films of $x\leq0.70$ were grown by NH_3-MBE and $x\geq0.73$ were grown by MOVPE.

Downloaded 31 Aug 2011 to 130.34.134.250. Redistribution subject to AIP license or copyright; see http://jap.aip.org/about/rights_and_permissions

III. THEORETICAL ANALYSIS

To quantitatively explain the experimental findings, the energies and oscillator strengths of the interband transitions involving three separate VBs were calculated using the Bir–Pikus Hamiltonian,[27] taking the anisotropic strains into account. At the Γ point, the states at the conduction band minimum (CBM) have an atomic *s* orbital with wave functions of $|S\rangle$ symmetry. The three VB maximum (VBM) states have atomic *p* orbitals with wave functions of a combination of $|X\rangle$, $|Y\rangle$, and $|Z\rangle$ symmetries. For simplicity, excitonic effects were neglected in the calculation. The Hamiltonian for the strain dependence of VB is given by the following 6×6 matrix

$$H=\begin{bmatrix} F & 0 & -H^* & 0 & K^* & 0 \\ 0 & G & \Delta & -H^* & 0 & K^* \\ -H & \Delta & \lambda & 0 & I^* & 0 \\ 0 & -H & 0 & \lambda & \Delta & I^* \\ K & 0 & I & \Delta & G & 0 \\ 0 & K & 0 & I & 0 & F \end{bmatrix},$$

where

$$F=\Delta_1+\Delta_2+\lambda+\theta,$$

$$G=\Delta_1-\Delta_2+\lambda+\theta,$$

$$H=i(A_6k_zk_+A_7k_++D_6\epsilon_{z+}),$$

$$I=i(A_6k_zk_+-A_7k_++D_6\epsilon_{z+}),$$

$$K=A_5k_+^2+D_5\epsilon_+,$$

$$\lambda=A_1k_z^2+A_2k_\perp^2+D_1\epsilon_{zz}+D_2(\epsilon_{xx}+\epsilon_{yy}),$$

$$\theta=A_3k_z^2+A_4k_\perp^2+D_3\epsilon_{zz}+D_4(\epsilon_{xx}+\epsilon_{yy}),\quad \Delta=\sqrt{2}\Delta_3,$$

$$k_\perp^2=k_x^2+k_y^2,\quad k_+=k_x+ik_y,$$

$$\epsilon_{z+}=\epsilon_{xz}+i\epsilon_{yz},\quad \epsilon_+=\epsilon_{xx}-\epsilon_{yy}+2i\epsilon_{xy}. \tag{1}$$

The parameters D_j $(j=1-6)$ denote the deformation potential constants for the VB and A_j $(j=1-7)$ are Luttinger parameters, and $\epsilon_{\ell m}$ and $k_\ell(\ell,m=X_1,X_2,X_3)$ are the strain and wave-vector components, respectively. Here we assume that nondiagonal elements of the strain tensor are zero. $\Delta_1=\Delta_{\rm sr}$ is the crystal field splitting, while $3\Delta_2=3\Delta_3=\Delta_{\rm so}$ are the spin-orbit splitting under quasicubic approximation. The basis functions of Bir–Pikus Hamiltonian are $(1/\sqrt{2})|X+iY,\alpha\rangle$, $(1/\sqrt{2})|X+iY,\beta\rangle$, $(1/\sqrt{2})|X-iY,\alpha\rangle$, $(1/\sqrt{2})|X-iY,\beta\rangle$, $|Z,\alpha\rangle$, and $|Z,\beta\rangle$. Here $|\alpha\rangle$ and $|\beta\rangle$ denote the spin-wave functions corresponding to up spin and down spin. The method described here is universal, and Bhattacharyya *et al.*[26] have also used the same approach to calculate the electronic states of *m*-plane (Al, In, Ga)N alloys.

The exciton transition energies are obtained from the band energies and exciton binding energy

TABLE I. Material parameters of GaN and AlN.

	GaN[a]	AlN[b]
E_g at 10 K (eV)	3.504	6.095
$\Delta_{cr}=\Delta_1$ (meV)	16	−152.4
$\Delta_{so}=3\Delta_2=\Delta_3$ (meV)	22	18.9
$m_\parallel^e/m_0$	0.2	0.32
$m_\perp^e/m_0$	0.18	0.28
A_2	−0.91	−0.28
A_4	−2.83	−1.84
C_{11} (GPa)	390	396
C_{12} (GPa)	145	137
C_{13} (GPa)	106	120
D_1 (eV)	−41.4	−17.2
D_2 (eV)	−33.3	7.9
D_3 (eV)	8.2	8.19
D_4 (eV)	−4.1	−4.1
D_5 (eV)	−4.7	−3.4

[a]Reference 14.
[b]Reference 15.

$$E_j=E^*+E^c-E_j^v-E_{\rm ex}^b, \tag{2}$$

where $E^*=E_g+\Delta_1+\Delta_2$. The parameters E_g, E^c, E_j^v, and $E_{\rm ex}^b$ are the bandgap energy, the CBM energy, the VBM energies, and the exciton binding energy, respectively. The $E_{\rm ex}^b$ values for the *A*, *B*, and *C* transition were set identical to 26 meV (Ref. 14) for GaN and 51.3 meV for AlN.[29]

The oscillator strength components for the transitions were obtained from momentum matrix elements $|\langle\Psi^{\rm CB}|p_\ell|\Psi^{\rm VB}\rangle|^2$ with $\ell=x$, y, and z. Here, $\langle\Psi^{\rm CB}|=\langle S|$ and $|\Psi^{\rm VB}\rangle=a_1|X\rangle+a_2|Y\rangle+a_3|Z\rangle$ represent the orbital parts of the CB and VB basis functions, respectively. The coefficients a_j were obtained by determining the eigenvectors of Hamiltonian. The *relative* values of $|\langle S|p_x|X\rangle|^2$, $|\langle S|p_y|Y\rangle|^2$, and $|\langle S|p_z|Z\rangle|^2$ are set unity under the quasicubic approximation $\Sigma_{i=1}^3 f_{i,\beta}=1$. The calculations started herein were carried out exclusively at $\mathbf{k}=0$, meaning that the 6×6 matrix was effectively treated as 3×3.

For the practical calculation on $Al_xGa_{1-x}N$ alloy films, the material parameters of end-point compounds, namely GaN and AlN, were taken from the literature, as shown in Table I. The parameters for the alloys were assumed to obey the Vegard's law and the bowing parameter for the bandgap energy of strain-free $Al_xGa_{1-x}N$ was chosen as 0.82 eV.[30] We use energy notations E_1, E_2, and E_3 hereafter because the crystal symmetry of the $Al_xGa_{1-x}N$ films suffering from anisotropic stresses is no longer C_{6v}^4.

The calculated relative oscillator strengths for the three interband transitions in $Al_{0.03}Ga_{0.97}N$ alloy are shown as functions of $\epsilon_{X_1X_1}$ and $\epsilon_{X_2X_2}$ by gray-scale contour plots in Fig. 3. For each E_1, E_2, and E_3 transition, the measured strain coordinate $(\epsilon_{X_1X_1},\epsilon_{X_2X_2})=(0.08\%,0.13\%)$ is plotted by a closed red circle on the panel exhibiting the calculated predominant polarization direction. As shown, the calculated polarization directions are X_3, X_1, and X_2 in order of decreasing electron energy. The result means that anisotropic strain induces a remarkable change in the electronic band structures: the ordering is already different from those of strain-free GaN. In the case of $Al_{0.70}Ga_{0.30}N$ alloy with

Downloaded 31 Aug 2011 to 130.34.134.250. Redistribution subject to AIP license or copyright; see http://jap.aip.org/about/rights_and_permissions

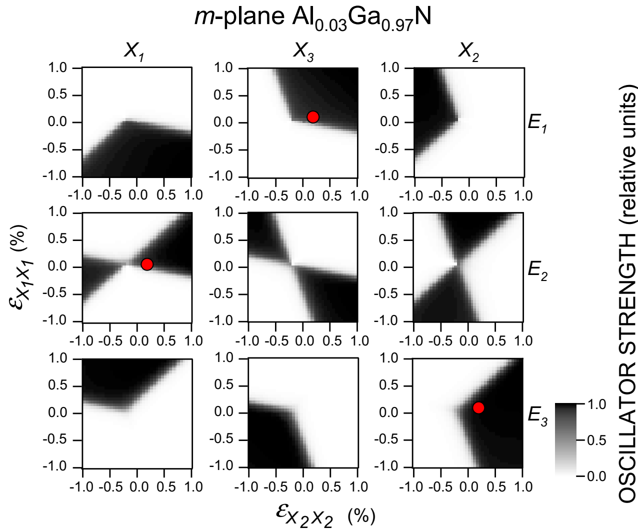

FIG. 3. (Color online) Relative oscillator strengths of E_1, E_2, and E_3 transitions for the m-plane $Al_{0.03}Ga_{0.97}N$ film as functions of in-plane strain coordinate $(\epsilon_{X_1X_1},\epsilon_{X_2X_2})$. Closed circles indicate the experimentally obtained in-plane strain coordinate $(\epsilon_{X_1X_1},\epsilon_{X_2X_2})=(0.08\%,0.13\%)$, which are plotted on the respective predominant polarization directions.

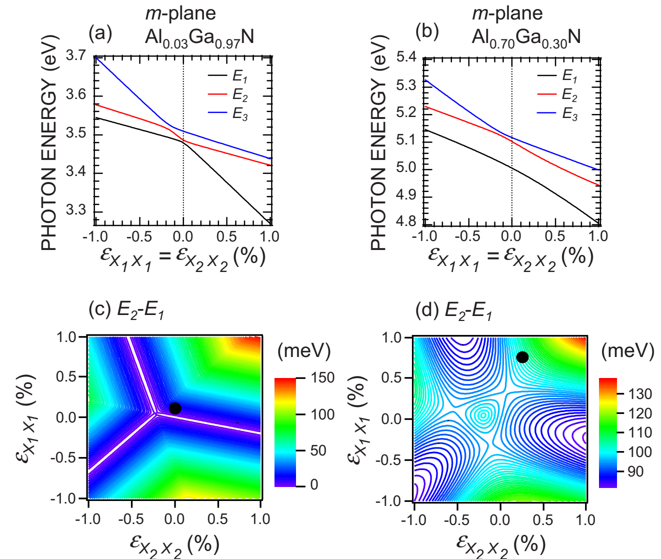

FIG. 5. (Color online) Calculated E_1, E_2, and E_3 exciton transition energies for the m-plane (a) $Al_{0.03}Ga_{0.97}N$ and (b) $Al_{0.70}Ga_{0.30}N$ films. The energy difference between E_2 and E_1, (E_2-E_1), as functions of in-plane strains $(\epsilon_{X_1X_1},\epsilon_{X_2X_2})$ for the m-plane (c) $Al_{0.03}Ga_{0.97}N$ and (d) $Al_{0.70}Ga_{0.30}N$ films. Closed circles indicate respective in-plane strains.

$(\epsilon_{X_1X_1},\epsilon_{X_2X_2})=(0.79\%,0.35\%)$, the polarization directions are calculated to be X_3, X_2, and X_1 in order of decreasing electron energy, as shown in Fig. 4. As revealed from Figs. 3 and 4, the polarization ordering of $Al_{0.70}Ga_{0.30}N$ was different from $Al_{0.03}Ga_{0.97}N$, and the oscillator strengths of $Al_{0.70}Ga_{0.3}N$ showed weaker contrast than $Al_{0.03}Ga_{0.97}N$. The reason for this will be explained later. Gil and Alemu[18] have reported a theoretical study on the electronic band structure of m-plane GaN under anisotropic biaxial strain. They predicted that E_1 and E_3 transitions were $E\perp c(X_1)$ polarized under large in-plane compressive strain. With respect to E_3 transition, their result differs from our calculated result for AlGaN alloys suffering from biaxial compressive strain (data not shown in this paper, because our AlGaN films basically

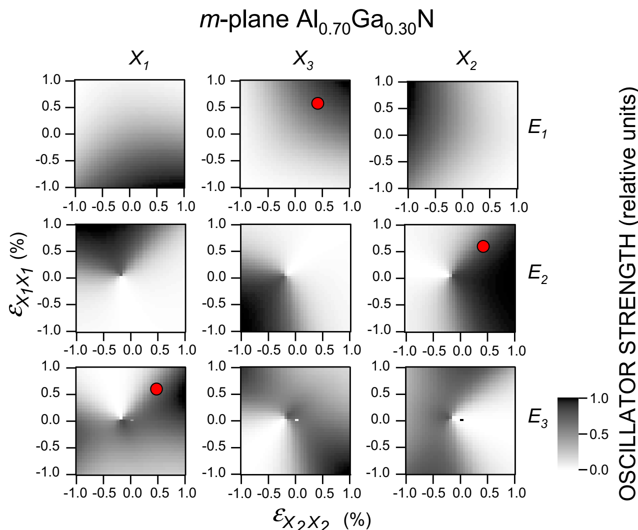

FIG. 4. (Color online) Relative oscillator strengths of E_1, E_2, and E_3 transitions as functions of in-plane strain coordinate $(\epsilon_{X_1X_1},\epsilon_{X_2X_2})$ for the m-plane $Al_{0.70}Ga_{0.30}N$ film. Closed circles indicate the experimentally obtained in-plane strain coordinate $(\epsilon_{X_1X_1},\epsilon_{X_2X_2})=(0.79\%,0.35\%)$, which are plotted on the respective predominant polarization directions.

suffered from in-plane tensile strains). The discrepancy might arise from the fact that we did not consider the excitonic effects. However, it is likely that their notation was different[19] from ours so that their m-plane would correspond to a-plane in our case, which might be the cause for this discrepancy. Similar arguments have been given by Bhattacharyya *et al.*[26]

The three exciton transition energies calculated for m-plane $Al_{0.03}Ga_{0.97}N$ and $Al_{0.70}Ga_{0.30}N$ films under isotropic in-plane strain $(\epsilon_{X_1X_1}=\epsilon_{X_2X_2})$ are shown in Figs. 5(a) and 5(b), respectively. In case of $Al_{0.03}Ga_{0.97}N$, the VB anticrossing immediately takes place when in-plane biaxial tensile strain is introduced. On the contrary, the VB anticrossing gradually takes place with increasing the tensile strain for $Al_{0.70}Ga_{0.30}N$. The latter result means that VBs are strongly hybridized, which gives rise to much lower oscillator strength contrast for $Al_{0.70}Ga_{0.30}N$, as shown in Fig. 4. The energy differences between E_1 and E_2 bands for the $Al_{0.03}Ga_{0.97}N$ and $Al_{0.70}Ga_{0.30}N$ films are shown using contour lines as functions of $\epsilon_{X_1X_1}$ and $\epsilon_{X_2X_2}$ in Figs. 5(c) and 5(d), respectively. Similar to Figs. 3 and 4, the measured strain coordinates are plotted by closed black circles. The E_2-E_1 values are predicted to be 6.2 and 106 meV for $Al_{0.03}Ga_{0.97}N$ and $Al_{0.70}Ga_{0.30}N$, respectively. Table II summarizes the polarization directions for E_1, E_2, and E_3 transitions and E_2-E_1 values calculated for m-plane $Al_xGa_{1-x}N$ suffering from experimentally obtained strain values. As shown, E_1 transition is X_3-polarized regardless of x. The result means that E_1 (exciton) emission is essentially undetectable from the surface normal. Apart from E_1, the polarization directions alter from X_1 to X_2 for E_2 emission (X_3 to X_2 for E_3 emission) between $x=0.25$ and 0.32. Assuming that the experimentally observed CL peaks originate from E_2 and E_3 transitions, the calculated prediction is consistent with the experimental results, as shown in Fig. 2(b). In Fig. 2(b), ρ

Downloaded 31 Aug 2011 to 130.34.134.250. Redistribution subject to AIP license or copyright; see http://jap.aip.org/about/rights_and_permissions

TABLE II. Calculated polarization directions for E_1, E_2, and E_3 transitions and energy differences between E_1 and E_2 band (E_2-E_1).

x	E_1	E_2	E_3	E_2-E_1 (meV)
0.00	X_1	X_3	X_2	7.7
0.03	X_3	X_1	X_2	6.2
0.12	X_3	X_1	X_2	48.4
0.25	X_3	X_1	X_2	96.9
0.32	X_3	X_2	X_1	124
0.58	X_3	X_2	X_1	88.4
0.70	X_3	X_2	X_1	106
0.73	X_3	X_2	X_1	108
1.00	X_3	X_2	X_1	142

values of *m*-plane $Al_xGa_{1-x}N$ films calculated using the oscillator strengths for the measured $(\epsilon_{X_1X_1}, \epsilon_{X_2X_2})$ coordinates are plotted as a function of x by open circles. As shown, the experimental data nearly agree with the calculated ones, except for the reduced ρ values for $x \leq 0.25$. The low ρ values may be due to the light depolarization caused by the high density surface striations along the *c*-axis, which had been disclosed using atomic force microscopy observation.[28] We must note in Fig. 2(a) that overall CL intensities for $x \geq 0.58$ were much weaker than those for $x \leq 0.32$. From Table II, it is obvious that E_2-E_1 increases with x. Therefore, Boltzmann distribution gives rise to very low hole populations in E_2 and E_3 bands in comparison with E_1 band for high x samples. This may be one of the reasons for the reduction in overall CL intensities for $x \geq 0.58$ at low temperature, where the nonradiative recombination channels are in principle frozen.

Finally, calculated E_2 transition energies (closed squares), CL peak energies (open circles), and their energy differences (ΔE) for the *m*-plane $Al_xGa_{1-x}N$ films are plotted as a function of x in Fig. 6. The ΔE value, which is similar to the Stokes-type shift, ranged between 3 and 577 meV for the alloys. These values were slightly larger than those reported for *c*-plane AlGaN films grown by MOVPE (100–250 meV).[30]

IV. CONCLUSION

Interband optical polarization characteristics of *m*-plane $Al_xGa_{1-x}N$ alloy films grown on the *m*-plane FS-GaN substrates were studied by means of polarized CL measurements and theoretical calculations. The predominant light polarization direction of the CL peak for the films suffering from in-plane anisotropic tensile stresses was shown to alter from $E \perp c(X_1)$ to $E \parallel c(X_2)$ between x=0.25 and 0.32. Theoretical analysis of the oscillator strengths of interband transitions and exciton transition energies was carried out using Bir–Pikus Hamiltonian, taking the anisotropic strain into account. The calculation predicted that the lowest energy transition (E_1) is X_3-polarized regardless of x, meaning that E_1 exciton emission is, in principle, undetectable from the substrate normal. Apart from E_1, the calculated polarization direction altered from X_1 to X_2 for E_2 transition and X_2 to X_1 for E_3 transition between $x=0.25$ and 0.32. Both the polarization ratios and overall CL intensities were quantitatively explained through the calculation. These achievements may cut open the way of designing nonpolar AlGaN device configurations.

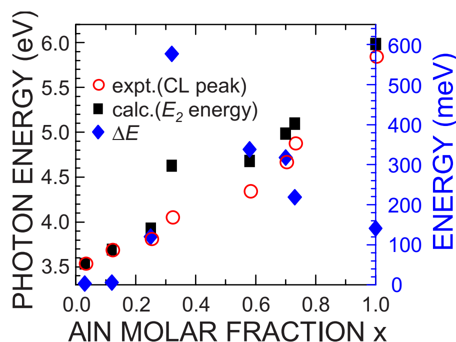

FIG. 6. (Color online) Calculated E_2 transition energies (closed squares), measured CL peak energies (open circles), and their energy differences (closed diamonds) for the *m*-plane $Al_xGa_{1-x}N$ films as a function of x.

ACKNOWLEDGMENTS

The authors would like to thank K. Fujito, H. Namita, T. Nagao, and H. Itoh of Mitsubishi Chemical Corporation for providing the *m*-plane FS-GaN substrates. This work was supported in part by Grant-in-Aids of CANTech, IMRAM, Tohoku University, Scientific Research in Priority Area No. 18069001 and Global COE program under MEXT, NEDO program by METI, Japan, and AOARD/AFOSR (FA2386-09-1-4013) monitored by G. Jessen.

[1]Y. Taniyasu, M. Kasu, and T. Makimoto, Nature (London) **441**, 325 (2006).
[2]S. F. Chichibu, A. Uedono, T. Onuma, S. P. DenBaars, U. K. Mishra, J. S. Speck, and S. Nakamura, Mater. Sci. Forum **590**, 233 (2008).
[3]P. Waltereit, O. Brandt, A. Trampert, H. T. Grahn, J. Menniger, M. Ramsteiner, M. Reiche, and K. H. Ploog, Nature (London) **406**, 865 (2000).
[4]M. D. Craven, P. Waltereit, J. S. Speck, and S. P. DenBaars, Appl. Phys. Lett. **84**, 496 (2004).
[5]T. Koida, S. F. Chichibu, T. Sota, M. D. Craven, B. A. Haskell, J. S. Speck, S. P. DenBaars, and S. Nakamura, Appl. Phys. Lett. **84**, 3768 (2004).
[6]J. S. Speck and S. F. Chichibu, MRS Bull. **34**, 304 (2009).
[7]K. Okamoto, H. Ohta, D. Nakagawa, M. Sonobe, J. Ichihara, and H. Takasu, Jpn. J. Appl. Phys., Part 2 **45**, L1197 (2006).
[8]M. C. Schmidt, K.-C. Kim, H. Sato, N. Fellows, H. Masui, S. Nakamura, S. P. DenBaars, and J. S. Speck, Jpn. J. Appl. Phys., Part 2 **46**, L126 (2007).
[9]K. Okamoto, H. Ohta, S. F. Chichibu, J. Ichihara, and H. Takasu, Jpn. J. Appl. Phys., Part 2 **46**, L187 (2007).
[10]M. C. Schmidt, K.-C. Kim, R. M. Farrell, D. F. Feezell, D. A. Cohen, M. Saito, K. Fujito, J. S. Speck, S. P. DenBaars, and S. Nakamura, Jpn. J. Appl. Phys., Part 2 **46**, L190 (2007).
[11]K. Fujito, K. Kiyomi, T. Mochizuki, H. Oota, H. Namita, S. Nagao, and I. Fujimura, Phys. Status Solidi A **205**, 1056 (2008).
[12]B. Gil, O. Briot, and R. L. Aulombard, Phys. Rev. B **52**, R17028 (1995).
[13]S. F. Chichibu, A. Shikanai, T. Azuhata, T. Sota, and S. Nakamura, Appl. Phys. Lett. **68**, 3766 (1996).
[14]A. Shikanai, T. Azuhata, T. Sota, S. Chichibu, A. Kuramata, K. Horino, and S. Nakamura, J. Appl. Phys. **81**, 417 (1997).
[15]H. Ikeda, T. Okamura, K. Matsukawa, T. Sota, M. Sugawara, T. Hoshi, P. Cantu, R. Sharma, J. F. Kaeding, S. Keller, U. K. Mishra, K. Kosaka, K. Asai, S. Sumiya, T. Shibata, M. Tanaka, J. S. Speck, S. P. DenBaars, S. Nakamura, T. Koyama, T. Onuma, and S. F. Chichibu J. Appl. Phys. **102**, 123707 (2007); **103**, 089901(E) (2008).
[16]K. Domen, K. Kondo, A. Kuramata, and T. Tanahashi, Appl. Phys. Lett. **69**, 94 (1996).
[17]T. Ohtoshi, A. Niwa, and T. Kuroda, J. Appl. Phys. **82**, 1518 (1997).

Downloaded 31 Aug 2011 to 130.34.134.250. Redistribution subject to AIP license or copyright; see http://jap.aip.org/about/rights_and_permissions

[18]B. Gil and A. Alemu, Phys. Rev. B **56**, 12446 (1997).
[19]A. Alemu, B. Gil, M. Julier, and S. Nakamura, Phys. Rev. B **57**, 3761 (1998).
[20]S.-H. Park and S.-L. Chuang, Phys. Rev. B **59**, 4725 (1999).
[21]S. Ghosh, P. Waltereit, O. Brandt, H. T. Grahn, and K. H. Ploog, Phys. Rev. B **65**, 075202 (2002).
[22]L. R. Ram-Mohan, A. M. Girgis, J. D. Albrecht, and C. W. Litton, Superlattices Microstruct. **39**, 455 (2006).
[23]S.-H. Park and D. Ahn, Appl. Phys. Lett. **90**, 013505 (2007).
[24]A. A. Yamaguchi, Jpn. J. Appl. Phys., Part 2 **46**, L789 (2007).
[25]A. A. Yamaguchi, Phys. Status Solidi C **5**, 2329 (2008).
[26]J. Bhattacharyya, S. Ghosh, and H. T. Grahn, Appl. Phys. Lett. **93**, 051913 (2008).
[27]G. L. Bir and G. E. Pikus, *Symmetry and Strain-Induced Effect in Semiconductors* (Wiley, New York, 1974).
[28]T. Hoshi, K. Hazu, K. Ohshita, M. Kagaya, T. Onuma, K. Fujito, H. Namita, and S. F. Chichibu, Appl. Phys. Lett. **94**, 071910 (2009).
[29]T. Onuma, T. Shibata, K. Kosaka, K. Asai, S. Sumiya, M. Tanaka, T. Sota, A. Uedono, and S. F. Chichibu, J. Appl. Phys. **105**, 023529 (2009).
[30]T. Onuma, S. F. Chichibu, A. Uedono, T. Sota, P. Cantu, T. M. Katona, J. F. Keading, S. Keller, U. K. Mishra, S. Nakamura, and S. P. DenBaars, J. Appl. Phys. **95**, 2495 (2004).

Downloaded 31 Aug 2011 to 130.34.134.250. Redistribution subject to AIP license or copyright; see http://jap.aip.org/about/rights_and_permissions